PROCEEDINGS OF ECOS 2023 - THE 36TH INTERNATIONAL CONFERENCE ON
EFFICIENCY, COST, OPTIMIZATION, SIMULATION AND ENVIRONMENTAL IMPACT OF ENERGY SYSTEMS
25-30 JUNE, 2023, LAS PALMAS DE GRAN CANARIA, SPAIN

Energetic and economic analysis of novel concentrating solar air heater using linear Fresnel collector for industrial process heat

Antonio Famiglietti[a], Antonio Lecuona[b],

[a] Universidad Politécnica de Madrid, Escuela Técnica Superior de Ingenieros Industriales, Departamento de Ingeniería Energética, Madrid, Spain, antonio_famiglietti@live.it, CA
[b] Universidad Carlos III de Madrid, Departamento de Ingeniería Térmica y de Fluidos, Leganés, Spain, lecuona@ing uc3m.es,

Abstract:

Industrial processes share a relevant portion of global energy consumption. Heat can be provided by solar thermal technologies aimed at the sustainable industry. A large variety of high energy-demanding industrial processes need hot air in the medium temperature range, provided by natural gas combustion or by electricity. Hot air is used as a medium in a large variety of processes such as drying, curing, and thermal treatments of several products and materials. Non-concentrating flat plate type solar collectors can directly heat air up to 100 °C while higher temperatures can be achieved using linear concentrating technology. In this study an innovative system using linear Fresnel collectors directly provides hot air for the industry up to 350 °C, avoiding the need for liquid heat transfer fluids. Accordingly, the installation is simplified, and lower installation and maintenance requirements are expected compared to other solar technologies. The present studies provide an energetic and economic analysis of the concentrating solar air heater, considering a medium-scale benchmark as a reference case in Southern Europe locations. The results indicate that the solar technology here presented can be economically competitive with other solar thermal solutions, having a huge potential for fossil fuel source replacement in hot air based industrial processes.

Keywords:

Solar heat for industrial processes, linear Fresnel; solar air heater, thermo-economic analysis; solar drying

1. Introduction

Industry consumes more than one-third of global energy [1] and is responsible for a quarter of global emissions. The greater industrial energy demand is heat, followed by electricity, provided almost totally from fossil fuel sources. Industrial heat consumption is estimated at around 85 EJ at the global level and is almost completely provided from fossil fuel. The total heat demand for low and medium temperature applications (< 400°C) accounts for 44 EJ, required by a large variety of industrial processes in any industrial sector.

Aiming at decarbonization, solar thermal technologies are good candidates for replacing fossil fuel technologies in industrial heat production. Besides costs, space availability, and solar resource, the application of Solar Thermal (ST) technologies to industrial heat is limited by their operating temperature range. Flat Plate Collectors (FPC) and Evacuated Tube Collectors (ETC) are suitable for low-temperature heat requirements (< 150 °C). Linear concentrating solar collectors are capable to provide heat at higher temperatures and efficiency than non-concentrating solar collectors e.g. [2] and they are receiving increasing attention for application to industrial processes [3]. Both Parabolic Trough Collectors (PTC) and Linear Fresnel Collectors (LFC) can provide heat in the medium temperature range (150 - 400 °C).

Hot air is used as a medium (working fluid) in a large variety of processes such as drying, curing, and thermal treatments of several products and materials [4]. Hot process air can be obtained by heating ambient air “indirectly” through a heat exchanger which is fed by a proper heat transfer fluid HTF (thermal oil, steam, hot water). HTF is heated by a conventional heat supply. Another common option is to heat air “directly” through a burner so that heated air and exhaust gases are mixed and utilized in the thermal process.

Linear concentrating collectors such as Parabolic Trough Collectors PTC and Linear Fresnel Collector LFC are commonly equipped with a heat transfer fluid HTF. Such are pressurized water, thermal oil, or steam, to

https://doi.org/10.52202/069564-0241

carry heat from the receiver tube that absorbs the concentrated solar irradiance and conveys it to the industrial process where it is needed. A heat exchanger is required to deliver heat to the processes when the heating medium differs from the HTF.

Their application for hot air production has been rarely documented, e.g. [6] and [7]. They use an indirect scheme where an HTF/air heat exchanger HX is needed to heat the process air.

An innovative scheme was proposed by [8] aiming at direct heating air inside the evacuated tube-type receiver of a linear concentrating collector. The theoretical analysis carried out revealed the feasibility of direct heating air in PTCs or LFCs under the appropriate range of solar field configuration. The pumping power needed for blowing air through the standard evacuated receiver tube rapidly grows with the solar field scale. To overcome this limitation, they propose to couple the solar field with an automotive turbocharger in a specific Brayton cycle configuration. The turbocharger allows operating with higher air density without consuming external auxiliary energy for pumping and blowing. A further numerical study [9] confirmed the technical feasibility of the turbo-assisted concentrating solar air heater, in that case, using a linear Fresnel Collector. A prototype has been built and tested allowing the full characterization of the small-scale linear Fresnel solar field available, using only air as the heat transfer fluid [10]. It operated assisted by a commercial turbocharger for air pumping [11].

The present study provides an energetic and economic analysis of the turbo-assisted concentrating solar air heater (T-SAH) applied to a generic process air heating case study, considering a -medium-scale benchmark as a reference.

2. Turbo-assisted concentrating solar air heater

According to the methodology detailed in [12], a benchmark solar field configuration is set. It is based on a commercial linear Fresnel collector [13], Fig.1. The solar field consists of 32 modules with 26.4 m^2 of primary mirrors area, forming a total active area of 845 m^2. The gross area of each module is 36 m^2 which gives a gross area occupied by the installation of 1270 m^2, including minimum spacing.

The LFC is equipped with a standard evacuated receiver tube. An automotive turbocharger joins a compressor c and a turbine e in a compact device with a common shaft, Fig.1. The compressor increases the air pressure up to 2 to 3.5 bar, according to operating conditions, before solar heating. Air velocities and stagnation pressure drops are minimized due to the increased density. After heating up to 450 - 550 °C, air expands through the turbine, which recovers the compressing power. This way no external auxiliary power is needed for air blowing. An auxiliary compressor is used for control and during starting transients only, with negligible yearly energy consumption.

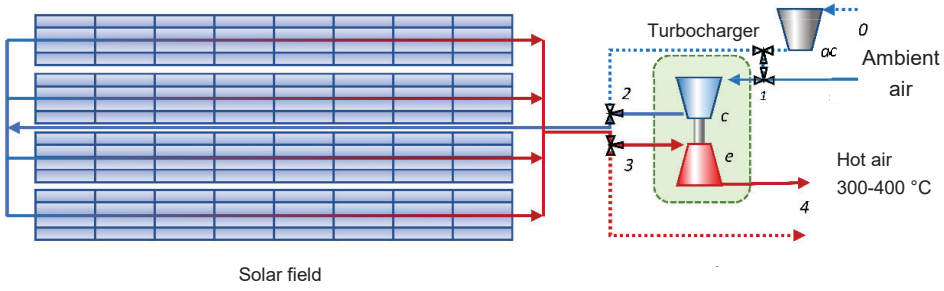

Figure. 1. Benchmark turbo-assisted concentrating solar air heater plant T-SAH.

Using a Typical Meteorological Year TMY, the delivered hot air stream and the thermal power delivered to the user are simulated for each hour of the year for a given location, resulting in a detailed yearly based assessment. The benchmark plant simulated is located in Madrid city, Spain.

Figure 2 shows the behavior of the system across a typical summer clear day through the main operating parameters involved. Fig.2 (a) reports the temperature profile during the day in the main points of the air circuit according to Fig. 1. It can be noticed as the delivered air temperature is relatively flat around T_4 =350 °C, thanks to the behavior of the turbocharger. The mass flow rate $\dot{m}_a$ varies according to the solar thermal power available. Pressurization imposed by the turbocharger reaches a pressure ratio of $\pi_c = \frac{p_2}{p_{amb}} = 3.5$ at midday,

https://doi.org/10.52202/069564-0241

which allows the minimization of pressure drops across the solar field and enables the turbine to drive the compressor without external aid (freewheeling). Accordingly, the required inlet turbine temperature goes up to 550 °C, while the receiver wall temperature T_w does not overcome its thermal limit ($T_{w,max} = 600$ °C). In spring and winter days both mass flow rate as well as operating temperature are lower, while the outlet air temperature is steadily above 300 °C.

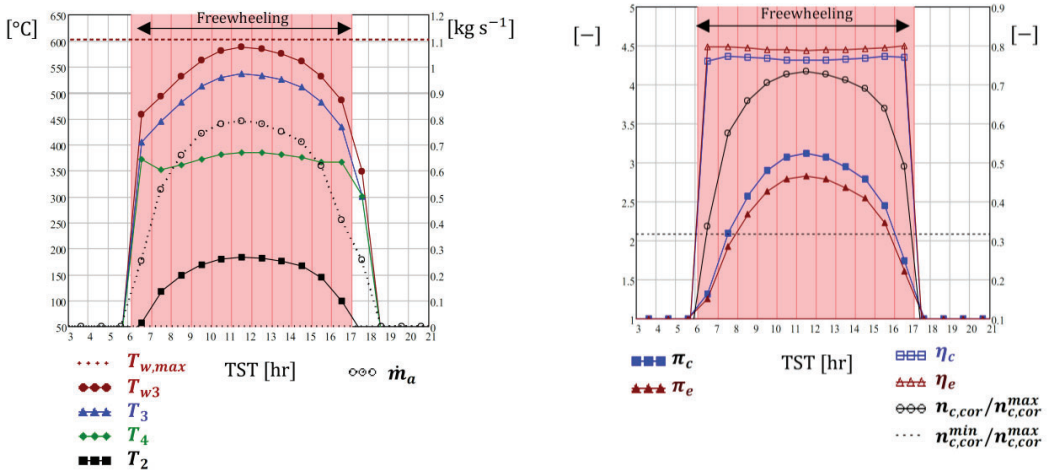

(a) (b)

Figure 2 Turbocharged Solar Air Heater T-SAH performances vs. true solar time TST during a clear summer day. Solar field orientation N-S. TST: true Solar Time; T, p: temperature and pressure according to Fig.1; T_{w3}: receiver wall temperature at tube outlet, $T_{w,max}$: maximum allowable receiver wall temperature; $n_{c,cor}$: turbocompressor (corrected) rotational speed; η_c: compressor efficiency; η_e: turbine efficiency; π_c: compressor pressure ratio; π_e: turbine pressure ratio; $\dot{m}_a$: mass flow rate; η_{th}: thermal efficiency.

Extending the simulation to the whole Typical Meteorological Year (TMY) annual results can be obtained. Oriented in the North-South direction and located in Madrid, Spain (40° 24' 59'' N, 3° 42' 9'' W) the solar field provides an annual energy yield $Q_a = 500$ MW h year^{-1} of thermal energy as hot air between 300 °C and 400 °C, working 2880 h year^{-1}, Tab.1.

Table 1. Yearly energetic performances

A_{tot}	m^2	845
h_{ON}	h	2880
Q_a	MW h y^{-1}	500
Q_a/A_{tot}	kW h y^{-1}m^{-2}	592.1
$Q_{a,u}$	MW h y^{-1}	491
Q_d	MW h y^{-1}	1600
SF_y	-	0.3

Although the previous results have general validity, in this analysis T-SAH delivers hot air to a specific thermal process, i.e. a medium-temperature drying process. The pre-existing conventional air heating device is assumed to be a natural gas burner, which is a common option in the industry. The burner sends to the process a mixture of combustion gases and air (referred to as hot air for simplicity) at the desired temperature, here assumed to be constant at 300 °C.

At least two options are viable for the integration of solar hot air into the existing air heating system: series and parallel integration with the natural gas burner, Fig.3. The integration concept chosen here is a parallel scheme

where T-SAH and the burner provide hot air for the process as in Fig.3(b). Whenever solar air flow is provided by the solar field it is totally sent to the process, having a priority over the burner airflow. The latter is adjusted by controlling the mass flow rate and temperature in order to meet the process requirements in terms of thermal power and air temperature. This way the solar air flow enables a reduction of burner thermal power, resulting in natural gas savings.

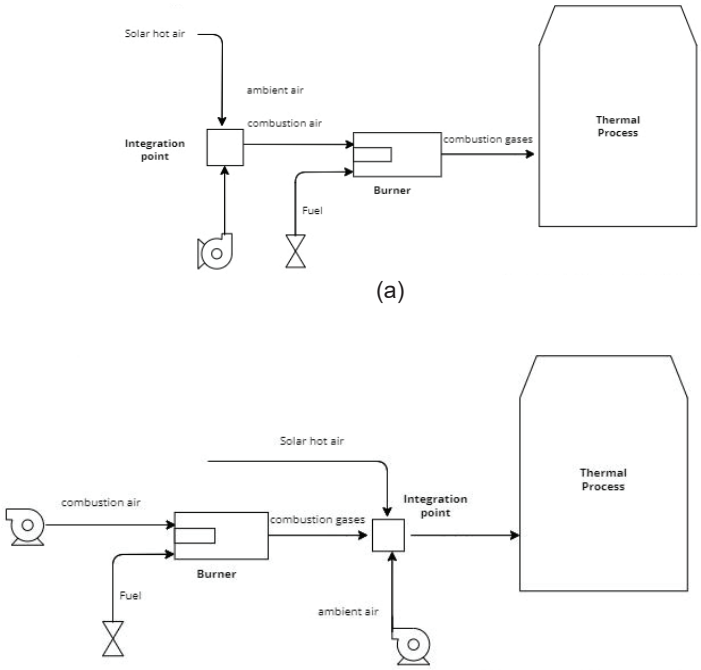

Figure. 3 Integration concept of T-SAH into air bases thermal process. i.e. drying: series integration (a); parallel integration (b).

The thermal load profile of the process depends on the specific factory, its requirements, and production schedule. Although any load profile is possible, some common patterns are recognized. A typical case is having a constant thermal load for continuous production. Another option is having a daily variation of thermal load according to the working hours of the factory. This can include or not the weekend among the working days. Here the thermal load $\dot{Q}_d$ is assumed to be 100% of the peak load $\dot{Q}_{d,pk} = 400$ kW, each day of the week including weekend days, from 7:00 a.m. to 6:00 p.m. During the rest of the hours thermal load is null.

The thermal load profile is shown in Fig.4 together with the solar production profile $\dot{Q}_a$ vs. the hours of the year for one week in summer Fig.4(a) and one week in winter Fig.4(b). The solar production interval and thermal load-interval are quite similar so that, even without thermal storage, the process can absorb almost all the solar thermal energy provided. The used thermal energy is in each hour $\dot{Q}_{a,u} = \min(\dot{Q}_d, \dot{Q}_a)$. On annual basis $\frac{Q_{a,u}}{Q_a} = 0.96$. The solar fraction SF is the ratio between the $\dot{Q}_{a,u}$ and $\dot{Q}_d$ in each time interval and indicates the amount of thermal load provided by solar. Fig. 4 reports on the second axis the SF for the selected weeks. It is clear that on summer days SF reaches up to 0.8, while it is much lower on typical winter days, $SF < 0.5$. On an annual basis, the solar fraction is $SF_y = 0.3$.

https://doi.org/10.52202/069564-0241

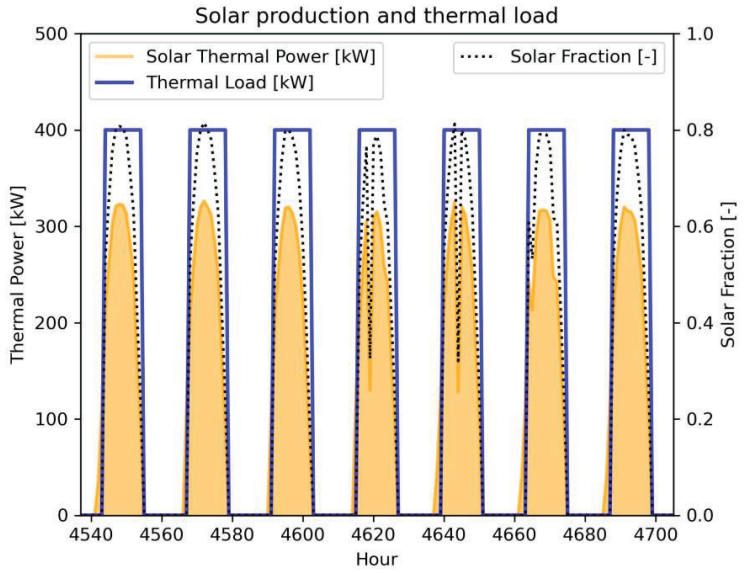

(a)

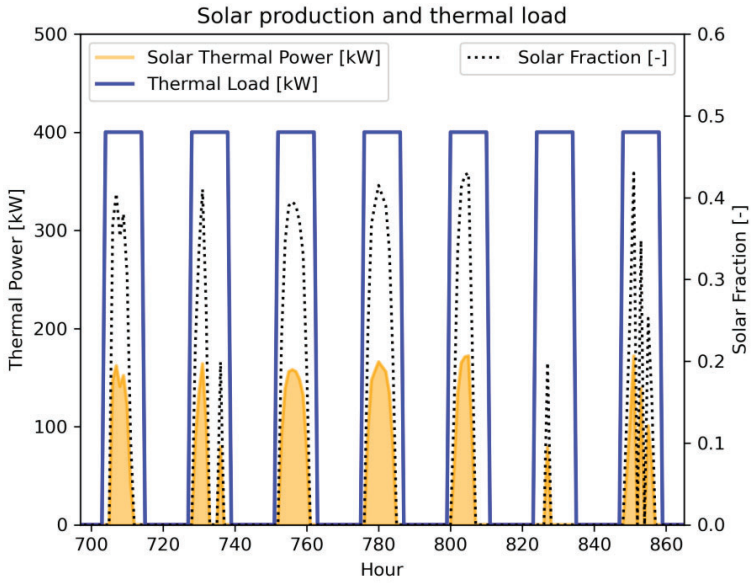

(b)

Figure 4. Solar production and thermal load weekly profiles: (a) typical summer week; (b) typical winter week.

3. Economy analysis

The economic analysis is carried out on the benchmark plant of Fig.1. Estimations of the installation costs CAPEX and operating cost OPEX are obtained on the grounds of the current stage of development of the technologies and products involved. Levelized cost of heat (LCOH) and discounted payback period (DPB) are used as the main economic parameters for the analysis.

Here it is assumed that solar-generated heat replaces the corresponding amount of convectional heat, generated by a natural gas burner.

The evaluation of conventional energy cost evaluation is non-trivial. Natural gas cost for industrial consumers varies by country, besides varying with the consumption volume of the factory and time. The price volatility has increased in Europe in recent months as a consequence of the geopolitical situation and supply uncertainties related to the major gas suppliers.

Eurostat [14] provides the natural gas price for "non-household" consumers across recent years in Europe. The "non-household" consumer definition includes industrial consumers and other large consumers with annual consumption above 1000 GJ (277 MWh), excluding powerplants and chemical process consumers. Non-household consumers are divided into six bands as reported in Tab.2.

As a general trend of the averaged value, since 2008 the price trend was increasing until 2013 reaching a peak at 42 €/MWh in the first half of 2013, then decreased down to 28 €/MWh in the first part of 2021. In 2021-2022 the prices have grown remarkably up to 65 €/MWh. Tab. 2 reports the recorded values for Spain and EU27 countries during the first semester of 2021 and 2022 when a large price variation occurred. These values are considered as a span for the price variation in the following economic study.

Table. 2. Non-household natural gas price including taxes by consumption bands, 2021-2022, €/MWh

		2021-S1		2022-S1	
Consumption band	Annual consumption	EU27	Spain	EU27	Spain
Band-I1	< 277 MWh	57.2	45.2	90.8	108.1
Band-I2	277 – 2 770 MWh	48.3	39.6	81.6	89
Band-I3	2 770 - 27 700 MWh	36.7	28.7	76.4	88.2
Band-I4	27 700 - 277 000 MWh	29.7	27.1	76.2	93.3
Band-I5	277 000 -1 108 000 MWh	27.7	28.1	87.7	92.1
Band-I6	> 1 108 000 MWh	26.6	26.1	97.7	89.2

3.1. LCOH

The LCOH is the cost of the generation of thermal energy (Heat), hence the minimum price at which it must be sold to recover the cost of installation (CAPEX) and the costs of operation and maintenance (OPEX, here named $C_{O\&M}$) during the lifetime of the plant. It is defined in an analogous way as the Levelized Cost of Energy $LCOE$ used for electricity production financial analysis. Here it is assumed that $LCOH$ is the cost of solar-generated heat, substituting the corresponding amount of convectional heat, generated by a conventional heating system.

According to IEA task 54, the $LCOH$ can be estimated as follows, considering constant annual discount rates r_{dis}:

$$LCOH = \frac{I_0 - S_0 + \sum_{n_y=1}^{N_y} \frac{C_{O\&M_{n_y}}(1-TR) - DEO_{n_y} TR}{(1+r_{dis})^{n_y}} - \frac{RV}{(1+r_{dis})^{N_y}}}{\sum_{n_y=1}^{N_y} \frac{E_{n_y}}{(1+r_{dis})^{n_y}}} \quad (1)$$

with I_0: initial investment and in due case discounted end-of-life replacements; S_0: subsidies on the installation; $C_{O\&M_{n_y}}$ yearly operation and maintenance cost, TR: corporate tax in %; DEO: asset depreciation; RV: residual value; E_{n_y}: Annual energy yield; N_y: Lifetime; r_{dis} discount rate % year-1.

The above expression results in the following simplified version when assuming $TR = 0$; $RV = 0$, and is used in this study.

$$LCOH = \frac{I_0 - S_0 + \sum_{n_y=1}^{N_y} \frac{C_{O\&M_{n_y}}}{(1+r_{dis})^{n_y}}}{\sum_{n_y=1}^{N_y} \frac{E_{n_y}}{(1+r_{dis})^{n_y}}} \quad (2)$$

Relevant parameters used are reported in Tab. 3. Initial investment $I_0 = C_{SF} + C_0$ has two main components.

https://doi.org/10.52202/069564-0241

The solar field $C_{SF} = A_{tot} C_{SFu}$ cost plays the major role compared to other costs C_0, including hydraulic and auxiliary equipment, control, and instrumentation. Solar field cost represents close to 90% of the initial investment. Although this is a common feature in solar installation, here is more evident since the auxiliary equipment is simplified thanks to the novel layout of direct air heating. The heat transfer fluid HTF and air/HTF heat exchanger are avoided with their related installation and maintenance costs.

Table 3. Financial parameters

Discount rate	r_{dis}	5%
Operation and Maintenance	$C_{O\&M}$	1% of initial investment I_0
Lifetime	N_y	25 years
Solar field cost per m^2	C_{SFu}	380-580 €/m2
Other costs (hydraulic and auxiliary equipment, control and instrumentation…)	C_0	50 000 €

The LCOH is obtained as a function of unitary solar field cost C_{SFu}, for the benchmark case having an annual energy yield of $Q_{a,u} = 491$ MWh. It ranges between 61 €/MWh ($C_{SFu} = 380 \frac{€}{m^2}$) and 89 €/MWh ($C_{SFu} = 580 \frac{€}{m^2}$), with an average of 75 €/MWh ($C_{SFu} = 480 \frac{€}{m^2}$). The comparison with natural gas costs suggests as the adoption of T-SAH can be economically viable when natural gas cost stays above its average value.

Fig. 5 shows the obtained LCOH in comparison with the natural gas cost for different consumption bands as in Tab. 2. The LCOH is higher than the minimum natural gas price so economic convenience is not guaranteed. When the natural gas prices are higher (as in 2022) the solar heat can be competitive or even cheaper. Besides, the smaller consumers suffer higher prices which can facilitate the adoption of solar energy solutions, but they must be able to consume all the solar heat provided by a flexible heat demand or via storage, not considered in this analysis. Considering the subsidies on the initial investment LCOH decreases: 48 €/MWh with $C_{SFu} = 480 \frac{€}{m^2}$ and the percentage of subsidies on the initial investment of $s_0 = \frac{S_0}{I_0} = 40\%$.

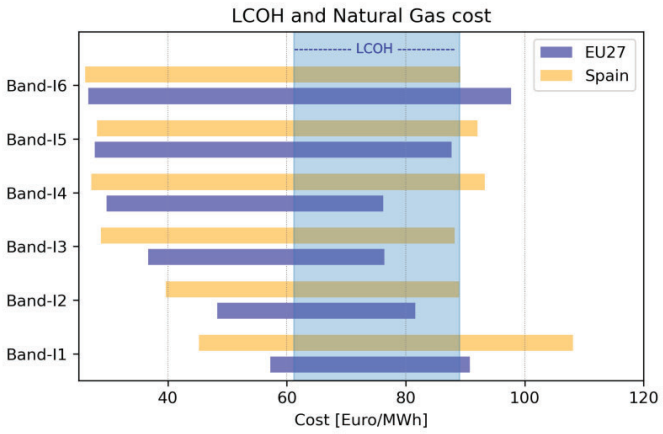

Figure 5. LCOH and natural gas cost span (2021-2022) in EU27 and Spain.

3.2. DPB

Discounted payback time DPB accounts for the time value of the money, hence it discounts the actual cash inflow for each year at the defined discount rate. Discounted Payback time DPB also depends on the cost of the conventional energy that is being replaced. A simplified equation is used for its evaluation are Eqs. (3) - (4). Yearly cash flow CF comes from natural gas costs avoided C_{NG} and operation and maintenance costs

$C_{O\&M}$. The conversion efficiency of natural gas burner is assumed unitary.

$$CF = \mathrm{Q_{a,u}} C_{\mathrm{NG}} - C_{O\&M} \tag{3}$$

$$DPB = \frac{\ln\left(\frac{CF}{CF - r_{dis}\,(I_0 - S_0)}\right)}{\ln(1 + r_{dis})} \tag{4}$$

Due to the variability of the conventional energy source price, it is convenient to show the DPB as a function of that price, as in Fig. 6. Three curves are shown representing the DPB assuming a solar field cost $C_{SFu} = 580\,\frac{€}{\mathrm{m^2}}$, $C_{SFu} = 480\,\frac{€}{\mathrm{m^2}}$, $C_{SFu} = 380\,\frac{€}{\mathrm{m^2}}$ and considering the subsidies $s_0 = \frac{S_0}{I_0} = 40\%$ of the capital costs. The DPB holds relatively high values, above 10 years in the actual range of natural gas prices. A decrease in LFC cost is required to lower the DPB either with subsidies or not. Considering an average natural gas price of 65 €/MWh, $DPB = 12$ years is obtained when the LFC cost drops to $C_{SFu} = 250\,\frac{€}{\mathrm{m^2}}$, without subsidies on the initial investment.

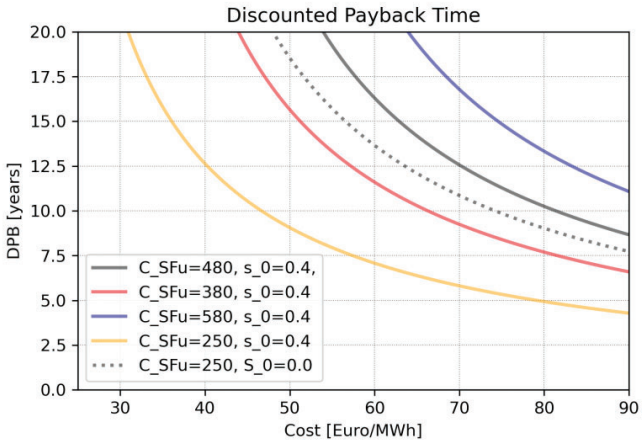

Figure 6. Discounted Payback Time *DPB* against the natural gas cost, for different unitary solar field costs and subsides percentage on the initial investment $s_0 = S_0/I_0$.

Conclusions

A novel layout for solar heat production for industrial processes has been studied from the economic perspective according to the energy yield utilization. The innovative concept uses concentrating linear Fresnel collectors to implement a solar air heater able to heat directly ambient air up to 300-400 °C for its usage in air-based thermal processes in the industry. An energetic analysis is carried out through numerical modeling of the solar heating system. A benchmark plant is configured and simulated across a typical meteorological year in Madrid city, Spain. The concentrating solar air heater is coupled with a thermal process, taking into account a parallel integration scheme and a given thermal load time profile. The simulation provides the annual performance of the solar facility in terms of energy provided and natural gas consumption avoided. An 845 m^2 solar field delivers to the process up to 500 MWh per year of thermal energy, corresponding to 30% of the consumption of the considered thermal process. The solar field allows for saving 52,000 Sm^3 of natural gas and 104 tons of CO_2 per year. The results indicate that the solar technology here presented can be competitive with other solar thermal solutions, having a huge potential for fossil fuel source replacement in hot air based industrial processes.

An economic analysis is carried out to evaluate the investment and operation costs of the solar system. The Levelized cost of Heat and Discounted Payback time indicates that the solution proposed can be competitive

https://doi.org/10.52202/069564-0241

with natural gas in the recent European price range, despite a reduction of solar field cost and sustained subsidies policy are required to improve economic feasibility.

Acknowledgments

This research was supported by the Industrial Ph.D. program of Comunidad de Madrid, Spain (BOCM Reference IND2017/ AMB7769) and “Ayudas Juan de la Cierva Formación de Ministerio de Ciencia e Innovación” funded by MCIN/AEI/10.13039/501100011033 and European Union “NextGenerationEU”/PRTR.

Nomenclature

Latin

A	Aperture surface area [m^2]
ac	Auxiliary compressor
CF	Cash flow
C_{NG}	Natural Gas cost
$C_{O\&M}$	Ôperation and Maintenance cost
C_{SFu}	Cost of solar field per m^2
C_0	Other costs
I_0	Initial Investment
$\dot{m}$	Air mass flow rate [kg s^{-1}]
n	Turbocharger rotating speed [rpm]
N_y	Lifetime [year]
p	Pressure [Pa]
$\dot{Q}$	Thermal power [W]
Q	Thermal energy [J]
r_{dis}	Discount rate
SF	Solar fraction
S_0	Subsidies
s_0	% of subsidies on I_0
T	Temperature [K, °C]
TST	True solar time [hr]

Greek

π	Pressure ratio [-]

Acronyms

HTF	Heat Transfer Fluid
DPB	Discounted payback
LCOH	Levelized cost of Heat
LFC	Linear Fresnel collector
PTC	Parabolic Trough Collector
SHIP	Solar Heat for Industrial Processes
T-SAH	Turbocharged Solar Air Heater

Subscripts

a	Air
amb	Ambient
a,u	Useful
c	Compression. Compressor
d	Demand, load
e	Expansion. Turbine
in	Inlet
ou	Outlet
tot	Total
w	Wall
0	Inlet from atmosphere
1	Compressor inlet
2	Compressor outlet
3	Turbine inlet
4	Turbine outlet

References

[1] “International Renewable Energy Agency (IRENA).” www.irena.org

[2] S. H. Farjana, N. Huda, M. A. P. Mahmud, and R. Saidur, “Solar process heat in industrial systems – A global review,” *Renewable and Sustainable Energy Reviews*, vol. 82, no. August 2017, pp. 2270–2286, 2018, doi: 10.1016/j.rser.2017.08.065.

[3] “SHIP Database.” http://ship-plants.info/

[4] A. K. Sharma, C. Sharma, S. C. Mullick, and T. C. Kandpal, “Solar industrial process heating: A review,” *Renewable and Sustainable Energy Reviews*, vol. 78, no. December 2016, pp. 124–137, 2017, doi: 10.1016/j.rser.2017.04.079.

[5] A. Saxena, Varun, and A. A. El-Sebaii, “A thermodynamic review of solar air heaters,” *Renewable and Sustainable Energy Reviews*, vol. 43, pp. 863–890, 2015, doi: 10.1016/j.rser.2014.11.059.

[6] S. Rehman, A. Ahmad, L. M. Alhems, and M. M. Rafique, “Experimental evaluation of solar thermal performance of linear Fresnel reflector,” *Journal of Mechanical Science and Technology*, vol. 33, no. 9, pp. 4555–4562, 2019, doi: 10.1007/s12206-019-0852-6.

[7] D. Pietruschka, I. Ben Hassine, M. Cotrado, R. Fedrizzi, and M. Cozzini, “Large Scale Solar Process Heat Systems -planning, Realization and System Operation,” *Energy Procedia*, vol. 91, pp. 638–649, 2016, doi: 10.1016/j.egypro.2016.06.223.

[8] A. Famiglietti, A. Lecuona-Neumann, J. Nogueira, and M. Rahjoo, “Direct solar production of medium temperature hot air for industrial applications in linear concentrating solar collectors using an open Brayton cycle . Viability analysis,” vol. 169, no. September 2019, 2020.

[9] A. Famiglietti, A. Lecuona, M. Ibarra, and J. Roa, “Turbo-assisted direct solar air heater for medium temperature industrial processes using Linear Fresnel Collectors. Assessment on daily and yearly basis,” *Energy*, vol. 223, 2021, doi: 10.1016/j.energy.2021.120011.

[10] A. Famiglietti and A. Lecuona, “Small-scale linear Fresnel collector using air as heat transfer fluid: Experimental characterization,” *Renewable Energy*, vol. 176, pp. 459–474, 2021, doi: 10.1016/j.renene.2021.05.048.

[11] A. Famiglietti and A. Lecuona, “Direct solar air heating inside small-scale linear Fresnel collector assisted by a turbocharger : Experimental characterization,” *Applied Thermal Engineering*, vol. 196, no. September, 2021, doi: 10.1016/j.applthermaleng.2021.117323.

[12] A. Famiglietti, A. Lecuona, M. Ibarra, and J. Roa, “Turbo-assisted direct solar air heater for medium temperature industrial processes using Linear Fresnel Collectors . Assessment on daily and yearly basis,” vol. 223, 2021.

[13] Solatom, “SOLAR STEAM FOR INDUSTRIAL PROCESSES.” http://www.solatom.com/

[14] “Eurostat.” https://ec.europa.eu/eurostat/

https://doi.org/10.52202/069564-0241